DRAFT
SAND2015-2728C
Proceedings of the ASME 2015 Pressure Vessels & Piping Division Conference
PVP2015
July 19-23, 2015, Boston, Massachusetts, USA

PVP2015-45424

OPTIMIZING MEASUREMENT OF FATIGUE CRACK GROWTH RELATIONSHIPS FOR CR-MO PRESSURE VESSEL STEELS IN HYDROGEN GAS

Brian Somerday
Sandia National Laboratories
Livermore CA, USA
bpsomer@sandia.gov

Paolo Bortot
Tenaris-Dalmine R&D
Dalmine, Italy
pbortot@tenaris.com

John Felbaum
FIBA Technologies
Millbury MA, USA
JohnFelbaum@fibatech.com

ABSTRACT

The objective of this study was to explore an approach for measuring fatigue crack growth rates (*da/dN*) for Cr-Mo pressure vessel steels in high-pressure hydrogen gas over a broad cyclic stress intensity factor (ΔK) range while limiting test duration, which could serve as an alternative to the method prescribed in ASME BPVC VIII-3, Article KD-10. Fatigue crack growth rates were measured for SA-372 Grade J and 34CrMo4 steels in hydrogen gas as a function of ΔK, load-cycle frequency (f), and gas pressure. The *da/dN* vs. ΔK relationships measured for the Cr-Mo steels in hydrogen gas at 10 Hz indicate that capturing data at lower ΔK is valuable when these relationships serve as inputs into design-life analyses of hydrogen pressure vessels, since crack growth rates in hydrogen gas approach rates in air in this ΔK range. The *da/dN* vs. f data measured for the Cr-Mo steels in hydrogen gas at selected constant-ΔK levels demonstrate that crack growth rates at 10 Hz do not represent upper-bound behavior, since *da/dN* generally increases as f decreases. Consequently, although fatigue crack growth testing at 10 Hz can efficiently measure *da/dN* over a wide ΔK range, these *da/dN* vs. ΔK relationships at 10 Hz cannot be considered reliable inputs into design-life analyses. A possible hybrid approach to efficiently establishing the fatigue crack growth rate relationship in hydrogen gas without compromising data quality is to measure the *da/dN* vs. ΔK relationship at 10 Hz and then apply a correction based on the *da/dN* vs. f data. The reliability of such a hybrid approach depends on adequacy of the *da/dN* vs. f data, i.e., the data are measured at appropriate constant-ΔK levels and the data include upper-bound crack growth rates.

INTRODUCTION

The Article KD-10 in Section VIII, Division 3 of the ASME Boiler and Pressure Vessel Code ("Special Requirements for Vessels in High Pressure Gaseous Hydrogen Transport and Storage Service") outlines a design-life analysis for high-pressure hydrogen vessels [1, 2]. This design-life analysis requires the fatigue crack growth rate (*da/dN*) vs. stress-intensity factor range (ΔK) relationship for the pressure-boundary material in the service environment, i.e., high-pressure hydrogen gas. One limitation in applying the ASME Article KD-10 design-life framework is the absence of *da/dN* vs. ΔK data for pressure vessel materials in high-pressure hydrogen gas. This data gap was recently addressed by performing fatigue crack growth rate measurements on SA-372 Grade J steel in hydrogen gas according to the ASME Article KD-10 [3]. Figure 1 displays these *da/dN* vs. ΔK relationships measured for three heats of SA-372 Grade J steel in 100 MPa hydrogen gas.

While the fatigue crack growth rate relationships in Fig. 1 enabled the design-life qualification of a hydrogen gas pressure vessel rated for 100 MPa, the data reflect a compromise to limit the duration of each test. Since the ASME Article KD-10 prescribes a load-cycle frequency of 0.1 Hz, the tests were designed with initial ΔK levels near 10 MPa $m^{1/2}$ to assure practical test durations. As a result, the *da/dN* vs. ΔK relationships do not include data at lower crack growth rates,

Sandia National Laboratories is a multi-mission laboratory managed and operated by Sandia Corporation, a wholly owned subsidiary of Lockheed Martin Corporation, for the U.S. Department of Energy's National Nuclear Security Administration under contract DE-AC04-94AL85000

i.e., in the lower ΔK range. When the *da/dN* vs. ΔK relationships in Fig. 1 were implemented in the design-life analysis for the 100 MPa hydrogen pressure vessel, the relationships were extrapolated to the lower ΔK range. It is likely that this extrapolation led to excessively conservative fatigue crack growth rates in the lower ΔK range, since the actual *da/dN* vs. ΔK relationship is expected to converge with the relationship measured in air at lower ΔK [4, 5].

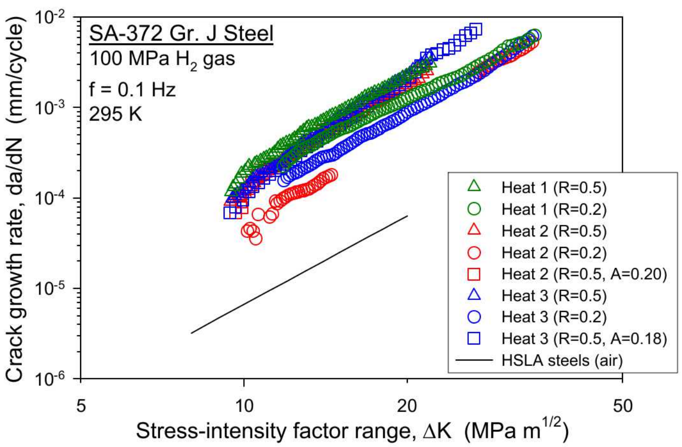

FIG. 1 FATIGUE CRACK GROWTH RATE RELATIONSHIPS FOR THREE SA-372 GR. J STEEL HEATS IN 100 MPa HYDROGEN GAS [3]

The objective of this study was to explore an alternative approach for measuring *da/dN* vs. ΔK relationships for Cr-Mo pressure vessel steels in high-pressure hydrogen gas, in which crack growth rates could be measured over a broad ΔK range while limiting the test duration. The approach involves measuring baseline *da/dN* vs. ΔK relationships at a relatively high load-cycle frequency (i.e., 10 Hz), which allows testing to progress through lower crack growth rates in a reasonable timeframe. However, since measured fatigue crack growth rates in hydrogen gas may be suppressed at higher load-cycle frequencies, *da/dN* vs. ΔK relationships measured at 10 Hz may be non-conservative. This aspect is addressed by supplemental measurements of fatigue crack growth rate as a function of load-cycle frequency (f) at selected constant-ΔK levels. These *da/dN* vs. f results can be applied to adjust the baseline *da/dN* vs. ΔK data to ensure the relationships represent upper-bound behavior.

NOMENCLATURE

a	Crack length or crack depth
a_o	Initial crack length or crack depth
da/dN	Crack growth rate (crack extension per load cycle)
f	Load-cycle frequency
B	Compact tension specimen thickness
B_n	Compact tension specimen net thickness
CT	Compact tension
K_{max}	Maximum stress-intensity factor
N	Number of load cycles
R	Load ratio (minimum load/maximum load)
S_u	Ultimate tensile strength
S_y	Yield strength
W	Compact tension specimen width
ΔK	Stress-intensity factor range

EXPERIMENTAL PROCEDURES

Two different Cr-Mo pressure vessel steels were featured in this study, SA-372 Grade J and 34CrMo4. These two steels were selected since both are qualified for seamless pressure vessel construction but represent two different strength ranges, i.e., the yield (S_y) and tensile (S_u) strengths were S_y = 760 MPa and S_u = 890 MPa for the SA-372 Grade J and S_y = 950 MPa and S_u = 1045 MPa for the 34CrMo4. These strength levels were attained by industrial quench-and-tempering heat treatments, following parameters specified in the ASME SA-372 and ISO 11120 standards for the SA-372 Grade J and 34CrMo4 steels, respectively. The heat treatments were applied to test rings removed from seamless pipes that serve as feedstock for manufacturing seamless pressure vessels. The wall thicknesses of the seamless pipes were 38 and 16 mm for the SA-372 Grade J and 34CrMo4 steels, respectively. The alloy compositions of the steels are listed in Table 1.

TABLE 1
COMPOSITION RANGES FOR Cr-Mo STEELS (WT%)*

Steel	Cr	Mo	Mn	Si	C
SA-372 Gr. J	0.99	0.18	0.93	0.28	0.49
34CrMo4	1.04	0.21	0.67	0.25	0.35

*Composition balance is Fe

Fatigue crack growth rate testing on the SA-372 Grade J and 34CrMo4 steels was performed following procedures in ASTM Standard E647-05 [6]. The test specimens were extracted from the seamless pipe products and designed according to the compact tension (CT) geometry. These specimens had the following nominal dimensions: thickness (B) = 12.7 mm, width (W) = 26.4 mm, and precrack-starter notch length = 5.3 mm. The specimens were designed with sidegrooves along the broad faces, which reduced the thickness in the crack plane (B_n) to 11.2 mm. The precrack-starter notch of the CT specimens was oriented parallel to the longitudinal axis of the seamless pipe.

The CT specimens were prepared for testing by first ultrasonically cleaning the as-machined specimens in isopropyl alcohol. Following procedures in ASTM Standard E647-05, a precrack was propagated from the starter notch in each specimen by applying cyclic loading. This fatigue precracking process was conducted in air under the following mechanical conditions: load-cycle frequency = 15 Hz, R ratio = 0.1, and final maximum stress-intensity factor (K_{max}) < 7.6 MPa m$^{1/2}$. The precrack was propagated a distance of approximately 2.8 mm from the notch tip to create a total precrack length-to-specimen width ratio (a_o/W) of 0.31.

Fatigue crack growth tests were performed on the Cr-Mo steel CT specimens in high-purity hydrogen (99.9999%) source gas at room temperature (approximately 295 K). This testing employed a custom-designed apparatus consisting of a pressure vessel inserted into the load train of a servo-hydraulic mechanical test frame. Each precracked CT specimen was placed in the pressure vessel and coupled to a pull rod penetrating through the bottom cover of the vessel (Fig. 2). The pressure vessel was equipped with spring-energized, Teflon® U-cup seals to prevent gas leakage between the pull rod and bottom cover bore. After the pressure vessel was assembled with the CT specimen inside, residual gas (e.g., air) was removed from the gas distribution manifold and pressure vessel by the following process: the pressure components were purged at least three times successively with high-purity helium gas (14 to 21 MPa pressure), evacuated once, then purged at least three more times successively with high-purity hydrogen gas (14 to 21 MPa pressure). Once these procedures were completed, the pressure vessel was filled with the source gas to the test pressure (10, 45, or 100 MPa), and each fatigue crack growth test was started within 72 h. The delay in starting the tests was necessary to ensure that hydrogen-induced changes in the strain gauge-based internal load cell output reached a constant saturation value, but these varying hydrogen-exposure times did not affect the fatigue crack growth data. Introducing gas to the pressure vessel did not result in net loads on the CT specimen due to pressure acting on the end of the pull rod, since a pressure balance chamber was designed into the vessel to ensure an equal and opposing force was applied to the pull rod.

At the termination of selected tests, hydrogen gas samples from the pressure vessel were collected in evacuated stainless steel bottles. The principal motivation for this sampling is recognition that oxygen and water vapor can contaminate the source gas, e.g., residual air cannot be completely removed from the pressure vessel and mixes with the 99.9999% hydrogen source gas. The post-test gas samples were analyzed for oxygen and water content at a commercial laboratory, revealing that concentrations of these species were less than 2.5 vppm and 18 vppm, respectively.

Two fatigue crack growth test methods were applied to the Cr-Mo steel CT specimens in hydrogen gas. In the first type of test, the CT specimens were subjected to cyclic loading between fixed minimum and maximum loads, in which the load ratio, R, was nominally 0.1 and the load-cycle frequency, f, was 10 Hz. This loading format led to increasing values of stress-intensity factor range, ΔK, as the crack extended. The purpose of these tests was to measure the baseline crack growth rate, da/dN, vs. stress-intensity factor range, ΔK, relationship. In the second type of test, the crack growth rate was measured at fixed values of ΔK. For these tests, the load ratio was constant (R = 0.1), but load-cycle frequency was varied in the range from 0.002 to 10 Hz. These tests were designed to measure the da/dN vs. f behavior. At each frequency, the crack growth rate was measured over approximately 1.3 mm of crack extension, and multiple measurements were made on a single specimen. For each of these specimens, crack growth segments at lower constant ΔK preceded those at higher constant ΔK.

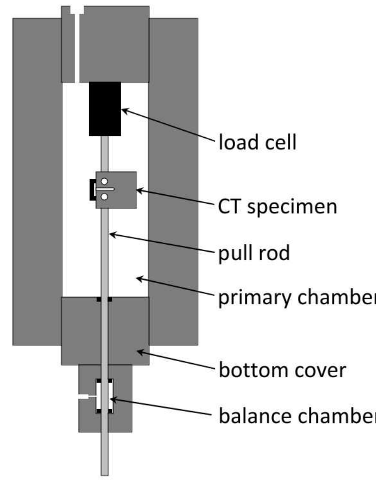

FIG. 2 SCHEMATIC OF CUSTOM PRESSURE VESSEL FOR FATIGUE CRACK GROWTH TESTING IN HYDROGEN GAS

For both fatigue crack growth test methods, the loading and unloading rates were programmed to be constant in each cycle (i.e., triangular loading wave form) using an internal load cell as the feedback transducer in the control loop. Since the Teflon® seals impose friction forces on the pull rod, the internal load cell ensured that loads applied to the specimen were measured directly. The crack-opening displacement was measured using a linear variable differential transformer (LVDT) attached to the front face of the CT specimen. Crack extension was quantified using the unloading compliance method. Load, crack-opening displacement, and crack length data were digitally recorded at crack extension intervals of 0.13 mm. A commercial fatigue crack growth software product was used to control both the programmed loading and data acquisition.

The type of data analysis depended on the fatigue crack growth test method. For the constant load amplitude tests, da/dN was calculated by applying the incremental polynomial method in ASTM E647-05 to the crack length, a, vs. load-cycle, N, data.[1] For each da/dN value, the associated ΔK was calculated from the crack length and load range at the mid-point of the evaluated crack length interval. For the constant-ΔK tests, the da/dN in each 1.3-mm crack extension segment was calculated from the slope of a line fit to the measured crack

[1] The crack length data furnished by the unloading compliance method were corrected based on post-test optical measurements of the precrack and final crack lengths from the fracture surfaces. The difference between the crack lengths determined from unloading compliance and optical measurements were approximately 10% for the precrack and < 5% for the final crack length. A routine in the analysis software linearly corrected the crack lengths calculated from unloading compliance so that the initial and final crack lengths equaled the optically measured values.

length vs. load-cycle data. In each constant-ΔK segment, initial crack extension often exhibited transient behavior before reaching steady state. The transient points were not included in the linear curve fit.

In addition to the fatigue crack growth tests in hydrogen gas, companion testing was performed in ambient air for the SA-372 Grade J steel. These CT specimens were prepared identically to those tested in hydrogen gas. The test parameters in air included constant load amplitude (R = 0.1), f = 15 Hz, and sinusoidal load-cycle wave form. The temperature and relative humidity in the ambient environment were approximately 295 K and 30 to 50%, respectively.

RESULTS AND DISCUSSION

Baseline *da/dN* vs. ΔK relationships were measured at 10 Hz for the SA-372 Grade J and 34CrMo4 steels in hydrogen gas at two different pressures (10 and 45 MPa). These baseline *da/dN* vs. ΔK responses for the two steels at both gas pressures (Fig. 3) are consistent with fatigue crack growth rate trends measured for other ferritic steels in hydrogen gas [4, 5]. In particular, the *da/dN* vs. ΔK relationships in Fig. 3 exhibit several characteristic fatigue crack growth rate regimes. In the lower ΔK range, fatigue crack growth rates in hydrogen gas approach crack growth rates in air. As ΔK increases, the crack growth rates in hydrogen gas rapidly accelerate, reaching levels that are approximately an order of magnitude higher than the crack growth rate in air. As ΔK continues to increase, each *da/dN* vs. ΔK curve features a markedly decreasing slope. Notably, the *da/dN* vs. ΔK relationships for the 34CrMo4 steel are virtually independent of hydrogen gas pressure, but fatigue crack growth rates for the SA-372 Grade J steel are higher at 45 MPa pressure compared to 10 MPa pressure. In addition, at the onset of hydrogen-accelerated fatigue crack growth, the 34CrMo4 steel exhibits higher crack growth rates compared to the SA-372 Grade J steel, but this difference in crack growth rates diminishes as ΔK increases.

One characteristic of the fatigue crack growth rate relationships in Fig. 3 that has significant implications for pressure vessel design-life analysis is the convergence of relationships in hydrogen gas and air at lower ΔK. In the absence of these lower-ΔK data, fatigue crack growth rate relationships must be extrapolated from data measured at higher ΔK. However, since crack growth rates in hydrogen gas approach rates in air as ΔK decreases, such an extrapolation can artificially inflate crack growth rates by as much as ten-fold, as illustrated in Fig. 1. Although the *da/dN* vs. ΔK measurements reflected in Fig. 3 appear to satisfy the objective of capturing the essential lower-ΔK data without prolonged testing times, it must be recognized that crack growth rates measured at 10 Hz may not represent upper-bound behavior. This aspect is addressed by measuring *da/dN* vs. load-cycle frequency, f, at selected constant-ΔK levels.

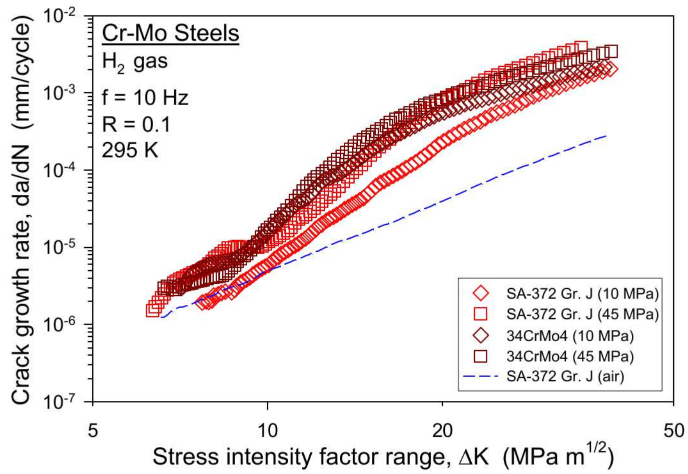

FIG. 3 FATIGUE CRACK GROWTH RATE RELATIONSHIPS MEASURED IN HYDROGEN GAS AT 10 HZ FOR SA-372 GR. J AND 34CrMo4 STEELS

Fatigue crack growth rates for the SA-372 Grade J and 34CrMo4 steels were measured as a function of load-cycle frequency at two constant-ΔK levels, 24 MPa m$^{1/2}$ and 15 MPa m$^{1/2}$. These measurements were performed in 10, 45, and 100 MPa hydrogen gas for the SA-372 Grade J steel but only in 10 and 45 MPa hydrogen gas for the 34CrMo4 steel. Another variation in testing parameters for the two steels was the maximum load-cycle frequency, which was 10 Hz for the SA-372 Grade J steel but only 1 Hz for the 34CrMo4 steel. The *da/dN* vs. f data are displayed in Fig. 4, revealing general trends with respect to load-cycle frequency, steel class, and hydrogen gas pressure. Considering load-cycle frequency, hydrogen-accelerated fatigue crack growth rates generally increase as frequency decreases. This trend is most pronounced for the 34CrMo4 steel in 45 MPa hydrogen gas at ΔK = 24 MPa m$^{1/2}$. The only apparent exceptions to this trend are for the 34CrMo4 steel at ΔK = 15 MPa m$^{1/2}$, in which *da/dN* is essentially independent of f; however, these data do not include measurements at 10 Hz. The *da/dN* vs. f data in Fig. 4 also allow a more compelling assessment of the relative hydrogen-accelerated fatigue crack growth susceptibilities for the two steels, since the data can provide upper-bound crack growth rates at lower load-cycle frequency. These upper-bound crack growth rates demonstrate that the higher-strength 34CrMo4 steel is generally more susceptible to hydrogen-accelerated fatigue crack growth than the lower-strength SA-372 Grade J steel. Under limited combinations of conditions, i.e., ΔK = 15 MPa m$^{1/2}$ and hydrogen gas pressure = 45 MPa, these upper-bound crack growth rates are nearly equal for the two steels. Regarding the effect of hydrogen gas pressure, Fig. 4 indicates that upper-bound crack growth rates generally increase as hydrogen gas pressure increases for both steels. One deviation from this trend is distinctly observed for the SA-372 Grade J steel at the highest gas pressures, in which crack growth rates are essentially equal at 45 and 100 MPa pressure.

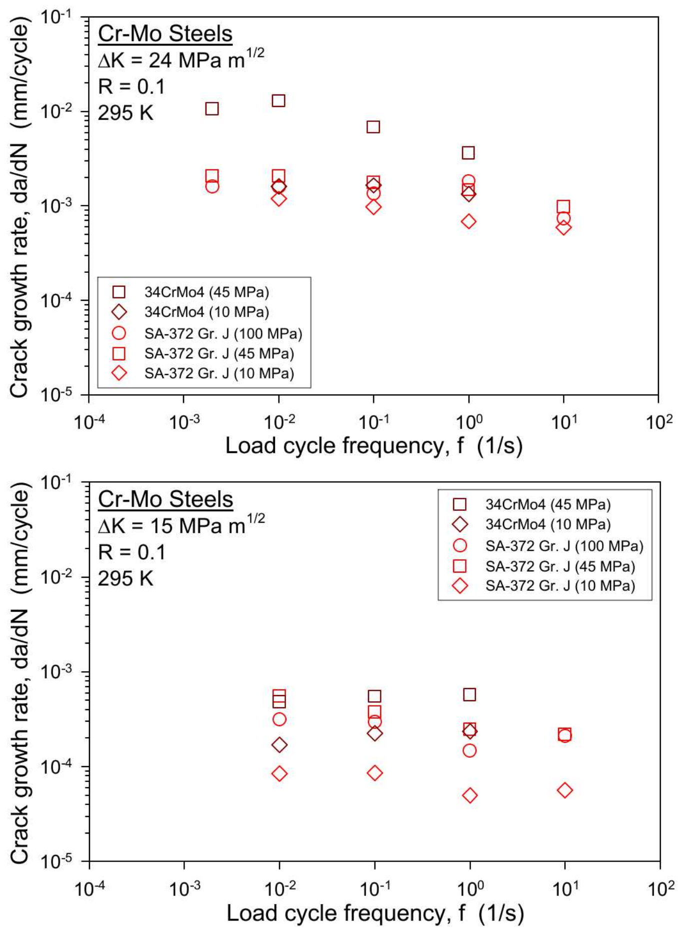

FIG. 4 FATIGUE CRACK GROWTH RATE VS. LOAD-CYCLE FREQUENCY MEASURED IN HYDROGEN GAS AT FIXED ΔK LEVELS FOR SA-372 GR. J AND 34CrMo4 STEELS

While the *da/dN* vs. *f* data in Fig. 4 are effective in revealing hydrogen-accelerated fatigue crack growth rates as a function of steel class and hydrogen gas pressure, the more important insight for pressure vessel design-life analysis is that crack growth rates are distinctly sensitive to load-cycle frequency. This trend of increasing crack growth rates as frequency decreases demonstrates that the *da/dN* vs. *ΔK* relationships measured at 10 Hz (Fig. 3) do not represent upper-bound crack growth rates. Consequently, such *da/dN* vs. *ΔK* relationships measured at high frequency cannot serve as reliable inputs into design-life analyses for hydrogen pressure vessels subjected to relatively infrequent pressure cycling.

Although the *da/dN* vs. *ΔK* relationships at 10 Hz do not represent the absolute solution to measuring fatigue crack growth rates over a broad *ΔK* range while limiting test duration, these relationships may serve as the foundation for a hybrid approach, as displayed in Fig. 5. In this figure, the *da/dN* vs. *f* data points at two different constant *ΔK* levels from Fig. 4 are superimposed on the baseline *da/dN* vs. *ΔK* relationships from Fig. 3. This composite set of data in Fig. 5 illustrates a concept for constructing the *da/dN* vs. *ΔK* relationship for design-life analysis, which balances test efficiency and data reliability. The baseline *da/dN* vs. *ΔK* relationships can be measured efficiently at 10 Hz, and these relationships indicate essential regimes that must be represented, i.e., the lower *ΔK* range, where crack growth rates in hydrogen gas approach those in air. Since *da/dN* vs. *ΔK* relationships must be considered as non-conservative at 10 Hz, the *da/dN* vs. *f* data measured at constant *ΔK* serve as a correction to the baseline curves. Data must be measured at multiple *ΔK* levels to provide the most reliable correction, and these *ΔK* levels can be selected based on key transition points in the baseline *da/dN* vs. *ΔK* relationships.

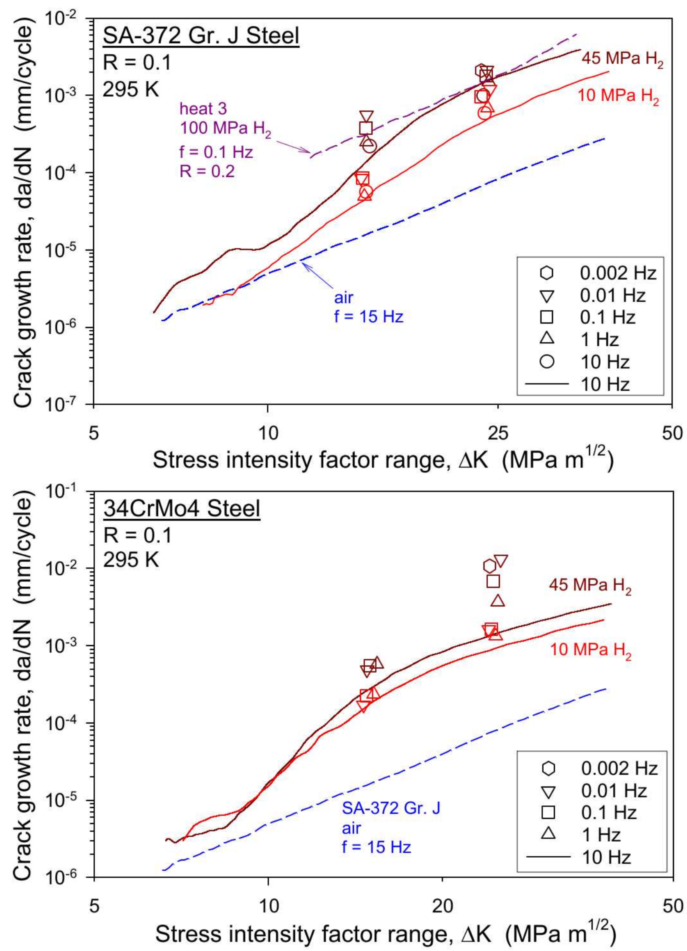

FIG. 5 FATIGUE CRACK GROWTH RATE VS. LOAD-CYCLE FREQUENCY DATA FROM FIG. 3 SUPERIMPOSED ON FATIGUE CRACK GROWTH RATE RELATIONSHIPS FROM FIG. 2. INCLUDED IN PLOT FOR SA-372 GR. J ARE da/dN VS. ΔK DATA FROM FIG. 1.

The *da/dN* vs. *f* data measured at only two constant-*ΔK* levels (e.g., 15 and 24 MPa $m^{1/2}$) may not be sufficient to correct the *da/dN* vs. *ΔK* relationship at 10 Hz. For example, included in Fig. 5 is one of the fatigue crack growth rate relationships presented in Fig. 1 for a similar heat of SA-372

Grade J steel ("heat 3"). This *da/dN* vs. *ΔK* relationship for SA-372 Grade J heat 3 was measured at a load-cycle frequency of 0.1 Hz, and Fig. 5 shows that crack growth rates for this steel are consistent with *da/dN* measured at 0.1 Hz under constant *ΔK* for the current SA-372 Grade J steel. One valuable insight revealed by including the data for SA-372 Grade J heat 3 in Fig. 5 is the notable dependence of the *da/dN* vs. *ΔK* slope transitions on load-cycle frequency, i.e., at the transition point where hydrogen-accelerated crack growth rates start to noticeably decrease at 10 Hz, high crack growth rates are sustained at 0.1 Hz. This suggests that additional data at lower constant-*ΔK* levels are required to reliably correct the baseline *da/dN* vs. *ΔK* relationship measured at 10 Hz.

The collective data in Fig. 5 indicate that correction factors applied to the baseline *da/dN* vs. *ΔK* relationships may not follow systematic trends. For example, the most significant correction to the baseline *da/dN* vs. *ΔK* relationships for the 34CrMo4 steel is at the higher *ΔK* in 45 MPa hydrogen gas. However, for the SA-372 Grade J steel, the most extensive corrections are required at the lower *ΔK* in 45 MPa hydrogen gas. The implication is that until an extensive database is developed, correction factors must be determined for each combination of steel class and hydrogen gas pressure.

One assumption implicit in the constructions displayed in Fig. 5 is that the *da/dN* vs. *f* data furnish upper-bound crack growth rates. In principle, the attainment of upper-bound crack growth rates can be confirmed from plots of *da/dN* vs. *f* at the selected constant-*ΔK* levels, i.e., Fig. 4. However, one factor that complicates interpretation of the *da/dN* vs. *f* data in Fig. 4 is that each *ΔK* level could not be ideally maintained at a constant value during consecutive crack-growth segments. For example, during the crack-growth segments in SA-372 Grade J steel at *ΔK* nominally equal to 24 MPa $m^{1/2}$, the *ΔK* levels actually varied from 24.2 to 23.4 MPa $m^{1/2}$ for each test in 10 and 45 MPa hydrogen gas. Since the crack growth rate is an exponential function of *ΔK*, even such modest variations in *ΔK* can have measurable effects on *da/dN*. Consequently, to compensate for the varying *ΔK* and its effect on crack growth rate, the *da/dN* data in Fig. 4 were normalized by crack growth rates at the respective *ΔK* levels from the baseline *da/dN* vs. *ΔK* relationships (Fig. 3). These normalized crack growth rate vs. load-cycle frequency data are plotted for the SA-372 Grade J and 34CrMo4 steels in Fig. 6.[2] Based on these normalized crack growth rate data, it appears that upper-bound crack growth rates are attained in the lower-frequency range for most tests, i.e., the normalized crack growth rate approaches a plateau as frequency decreases. The exception is the test for SA-372 Grade J under nominal constant *ΔK* = 15 MPa $m^{1/2}$ in 45 MPa hydrogen gas, in which the normalized crack growth rate continues to increase in the lower frequency range. In this case, additional *da/dN* data are needed at *f* less than 0.01 Hz to confirm upper-bound crack growth rates.

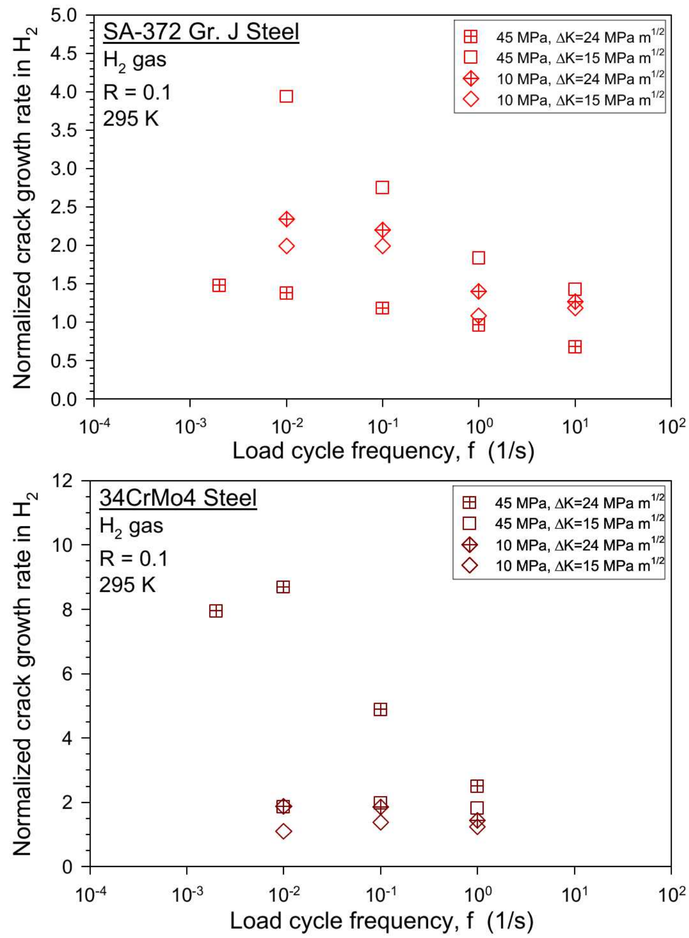

FIG. 6 NORMALIZED FATIGUE CRACK GROWTH RATE VS. LOAD-CYCLE FREQUENCY MEASURED IN HYDROGEN GAS AT FIXED ΔK LEVELS FOR SA-372 GR. J AND 34CrMo4 STEELS

CONCLUSIONS

- Fatigue crack growth rates, *da/dN*, were measured for the Cr-Mo pressure vessel steels SA-372 Grade J and 34CrMo4 in hydrogen gas as a function of stress-intensity factor range, *ΔK*, load-cycle frequency, *f*, and gas pressure for the purpose of exploring a more efficient approach to establishing the *da/dN* vs. *ΔK* relationship without compromising data quality.
- The *da/dN* vs. *ΔK* relationships measured for the Cr-Mo steels in hydrogen gas at 10 Hz indicate that capturing data at lower *ΔK* is valuable for design-life analyses of hydrogen pressure vessels, since crack growth rates in hydrogen gas approach rates in air in this *ΔK* range.
- The *da/dN* vs. *f* data measured for the Cr-Mo steels in hydrogen gas at selected constant-*ΔK* levels demonstrate that crack growth rates at 10 Hz do not represent upper-

[2] Normalized crack growth rates for SA-372 Grade J at 10 Hz do not equal 1.0 due to data variability, i.e., crack growth rates measured for the constant load amplitude test (Fig. 3) do not exactly equal crack growth rates measured for the constant-ΔK test at 10 Hz (Fig. 4).

bound behavior, since *da/dN* generally increases as *f* decreases. Consequently, although fatigue crack growth testing at 10 Hz can efficiently measure *da/dN* over a wide ΔK range, these *da/dN* vs. ΔK relationships at 10 Hz cannot be considered reliable inputs into design-life analyses.

- A possible hybrid approach to efficiently establishing the fatigue crack growth rate relationship in hydrogen gas without compromising data quality is to measure the *da/dN* vs. ΔK relationship at 10 Hz and then apply a correction based on the *da/dN* vs. *f* data. The reliability of such a hybrid approach depends on adequacy of the *da/dN* vs. *f* data, i.e., the data are measured at appropriate constant-ΔK levels and the data include upper-bound crack growth rates.

ACKNOWLEDGMENTS

The authors acknowledge K. Lee for assistance in performing the fatigue crack growth tests in high-pressure hydrogen gas. Support was provided by the U.S. Department of Energy Fuel Cell Technologies Office through the Hydrogen Safety, Codes and Standards sub-program element. Sandia National Laboratories is a multi-program laboratory managed and operated by Sandia Corp., a wholly owned subsidiary of Lockheed Martin Corp., for the U.S. Department of Energy's National Nuclear Security Administration under Contract DE-AC04-94AL85000.

REFERENCES

1. Rana, M.D., Rawls, G.B., Sims, J.R. and Upitis, E., 2007, "Technical Basis and Application of New Rules on Fracture Control of High Pressure Hydrogen Vessel in ASME Section VIII, Division 3 Code", PVP2007-26023, *2007 ASME Pressure Vessels and Piping Division Conference*, ASME, New York.
2. Sims, J.R., 2012, "Standards and Codes to Control Hydrogen-Induced Cracking in Pressure Vessels and Pipes for Hydrogen Gas Storage and Transport", *Gaseous Hydrogen Embrittlement of Materials in Energy Technologies*, R.P. Gangloff and B.P. Somerday, eds., Woodhead Publishing Ltd., pp. 177-192, Cambridge, UK.
3. Somerday, B., San Marchi, C., and Nibur, K., 2013, "Measurement of Fatigue Crack Growth Rates for SA-372 Gr. J Steel in 100 MPa Hydrogen Gas Following Article KD-10", PVP2013-97455, *2013 ASME Pressure Vessels and Piping Division Conference*, ASME, New York.
4. Suresh, S., and Ritchie, R.O., 1982, "Mechanistic Dissimilarities Between Environmentally Influenced Fatigue-Crack Propagation at Near-Threshold and Higher Growth Rates in Lower Strength Steels," Metal Science, **16**(11), pp. 529-538.
5. Macadre, M., Artamonov, M., Matsuoka, S., and Furtado, J., 2011, "Effects of Hydrogen Pressure and Test Frequency on Fatigue Crack Growth Properties of Ni-Cr-Mo Steel Candidate for a Storage Cylinder of a 70 MPa Hydrogen Filling Station", Eng. Fract. Mech., **78**(18), pp. 3196-3211.
6. ASTM E647-05, 2005, "Standard Test Method for Measurement of Fatigue Crack Growth Rates", ASTM International, West Conshohocken, PA.